

Electronic Supporting Information (ESI)

Optimizing electromagnetic wave absorption bandwidth of SiC/C aerogels using continuous multi-band absorption

Jingxiang Liu,^a Haoquan Hao,^a Yuheng Zhang,^a Lishu Wei,^a Yi Cui,^b Qinghe Jing,^b Shouqing Yan,^b Jie Guo,^b Zhijiang Wang^{*ac}

a MIIT Key Laboratory of Critical Materials Technology for New Energy Conversion and Storage,
School of Chemistry and Chemical Engineering, Harbin Institute of Technology, Harbin 150001, China.

b Zhalainuoer Coal Industry Co., Ltd, No.17, Yulin Street, Zhalainuoer Mining Area, Manzhouli City,
Hulun Buir 021410, China

c Inner Mongolia Haite Huacai Technology Co., Ltd, Management Committee Office Building, Jinqiao
Economic and Technological Development Zone, Hohhot 010000, China.

*Corresponding author.

E-mail address: wangzhijiang@hit.edu.cn

The calculation of attenuation constant

$$\alpha = \frac{\sqrt{2\pi}f}{c} \sqrt{(\mu''\epsilon'' - \mu'\epsilon') + \sqrt{(\mu''\epsilon'' - \mu'\epsilon')^2 + (\mu'\epsilon'' - \mu''\epsilon')^2}} \quad (1)$$

where f is the frequency and c is the speed of light in vacuum.

The calculation of reflection loss

Based on the transmission line theory, RL is calculated according to the following equation:

$$Z_{in} = Z_0 (\mu_r / \epsilon_r)^{1/2} \tan h[j(2\pi f d / c) ((\mu_r \epsilon_r)^{1/2})] \quad (2)$$

$$RL = 20 \log_{10} \left| \frac{Z_{in} - Z_0}{Z_{in} + Z_0} \right| \quad (3)$$

where Z_{in} and Z_0 are denoted as the impedance of free space and input impedance. f , d and c are the frequency of the EM waves, the thickness of the absorber and the speed of light in free space, respectively.

The calculation of impedance matching

$$M_Z = \frac{2Z_{in}'}{|Z_{in}|^2 + 1} \quad (4)$$

where Z_{in}' means the real normalized input impedance. The value of M_Z equal or close to 1.0 means the EMW can easily enter the material rather than reflection on the air or absorber interfaces.

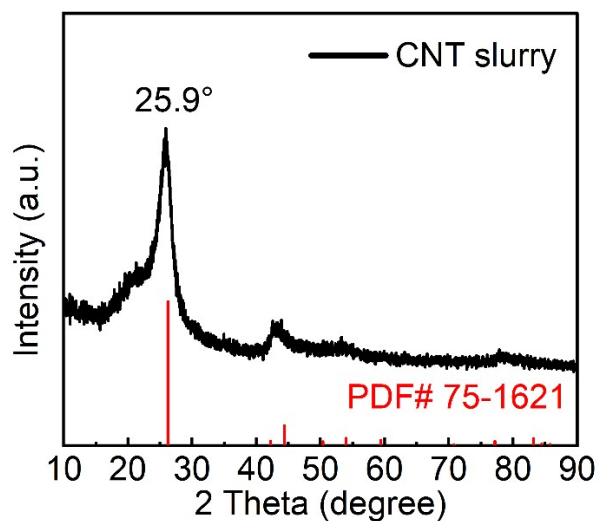


Fig. S1 XRD of CNT slurry after drying.

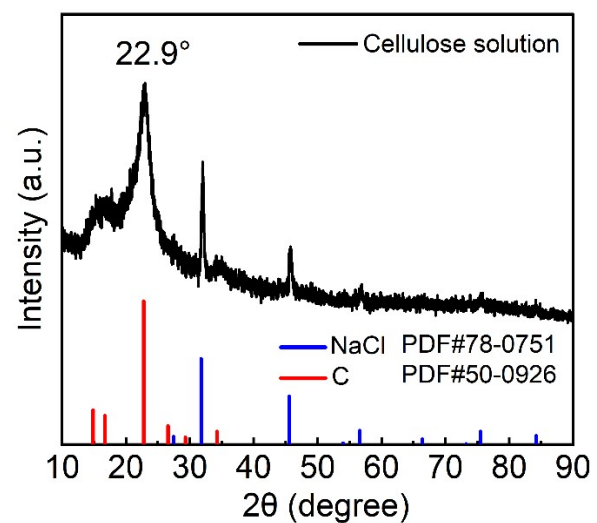


Fig. S2 XRD of cellulose solution after drying.

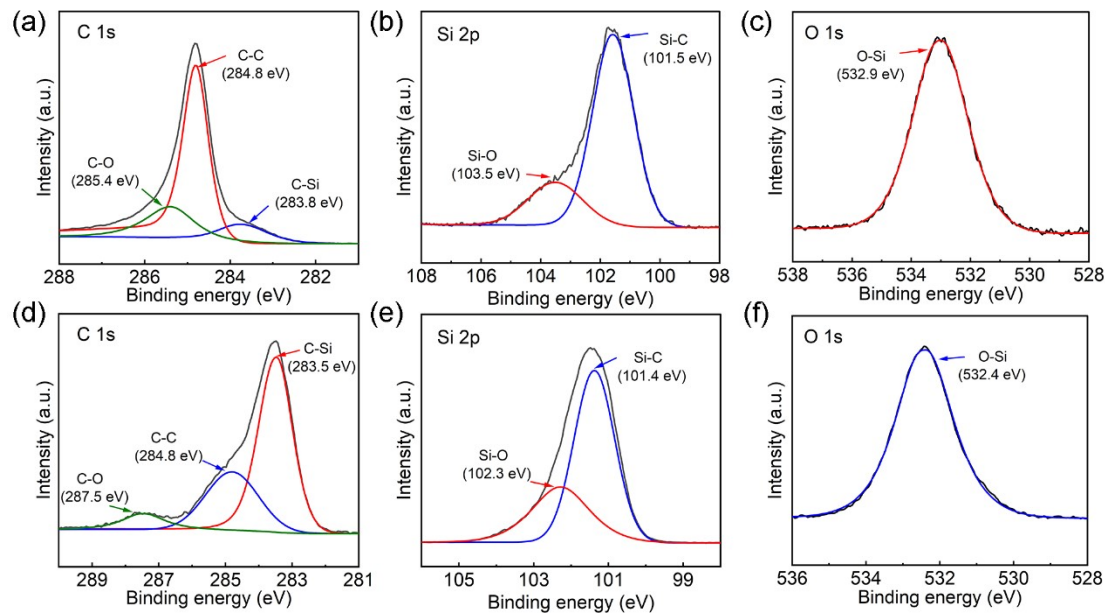


Fig. S3 XPS survey spectra of (a) C 1s, (b) Si 2p, and (c) O 1s regions of SN-1350.

XPS survey spectra of (d) C 1s, (e) Si 2p, and (f) O 1s regions of SN-1550.

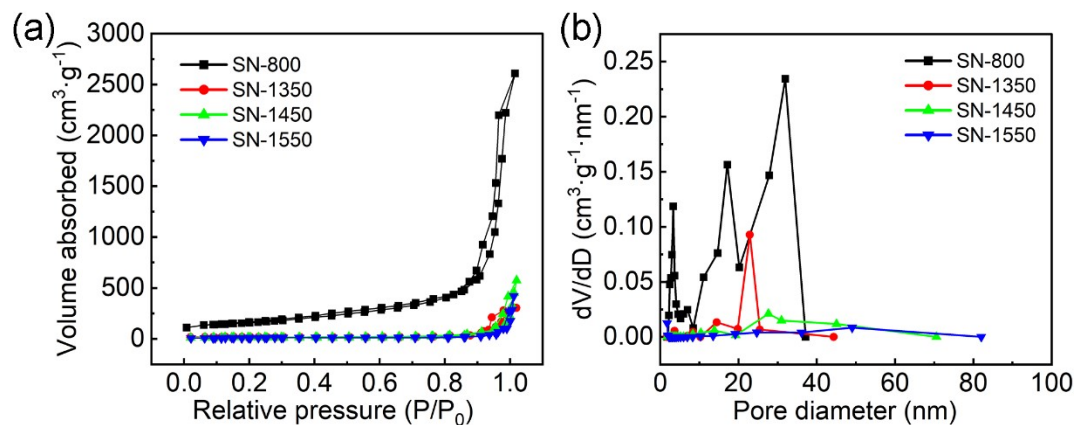


Fig. S4 (a) N₂ adsorption–desorption isotherms at 77 K and (b) pore size distributions of the samples.

Table. S1 Pore size and specific surface area of the samples.

Sample	Pore size (nm)	Specific surface area (m ² /g)
SN-800	28.2	559.3
SN-1350	25.3	73.3
SN-1450	45.4	62.6
SN-1550	63.9	40.5

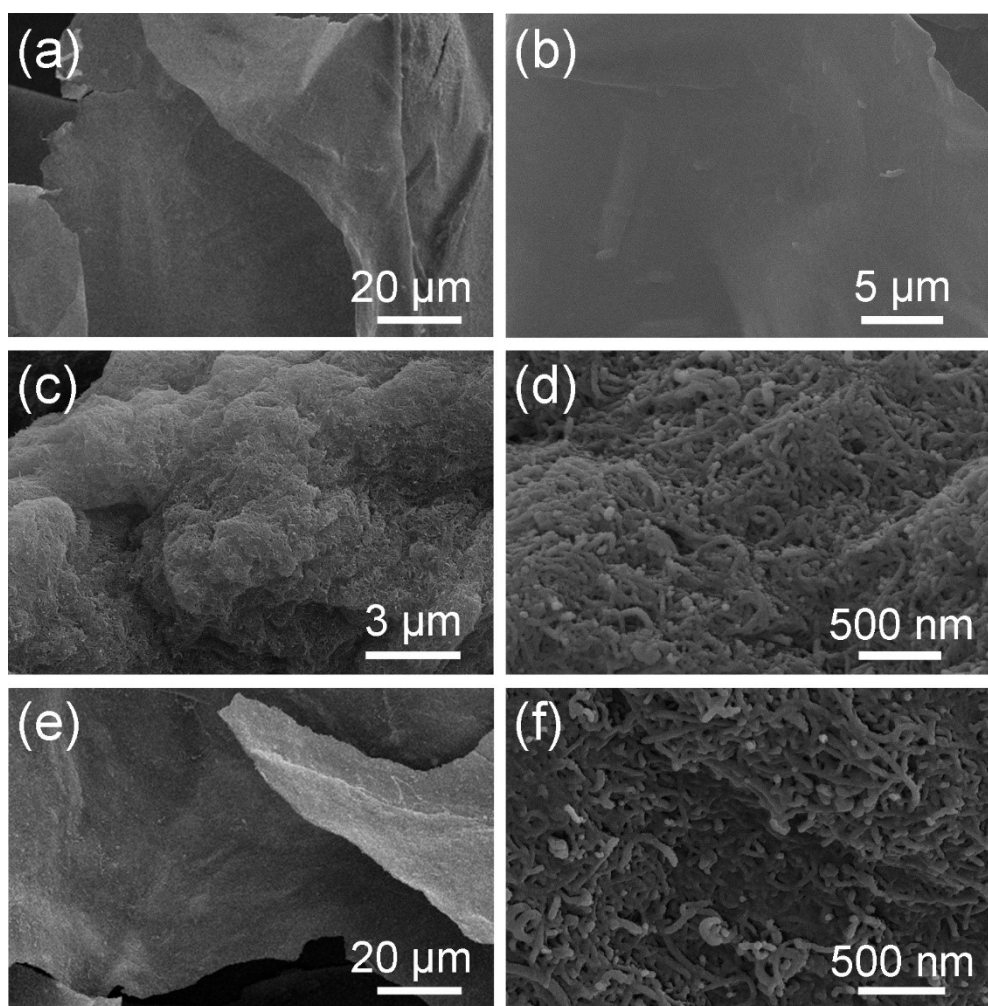


Fig. S5 SEM images of (a,b) cellulose microsheets, (c,d) CNTs slurry after drying, (e,f) SN-800.

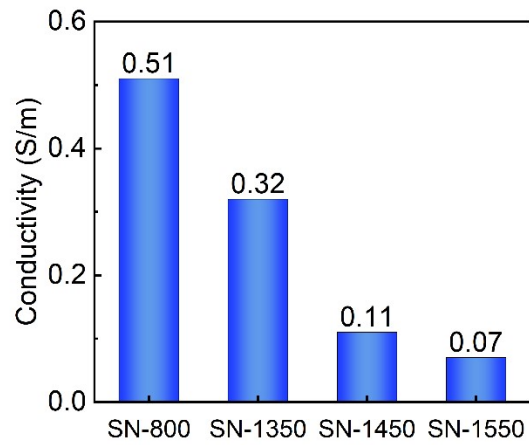


Fig. S6 The conductivity of the samples.

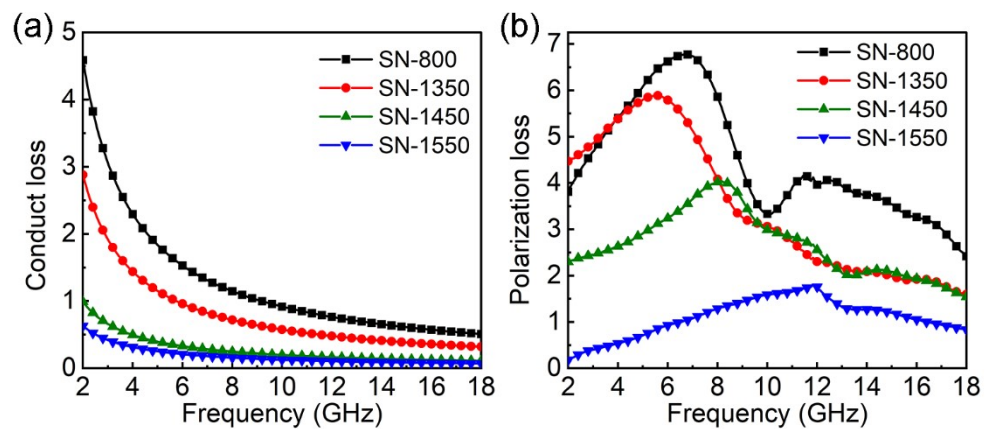


Fig. S7 Frequency dependence of the (a) conduction loss (ϵ_c''), and (b) polarization loss (ϵ_p'') of the samples.

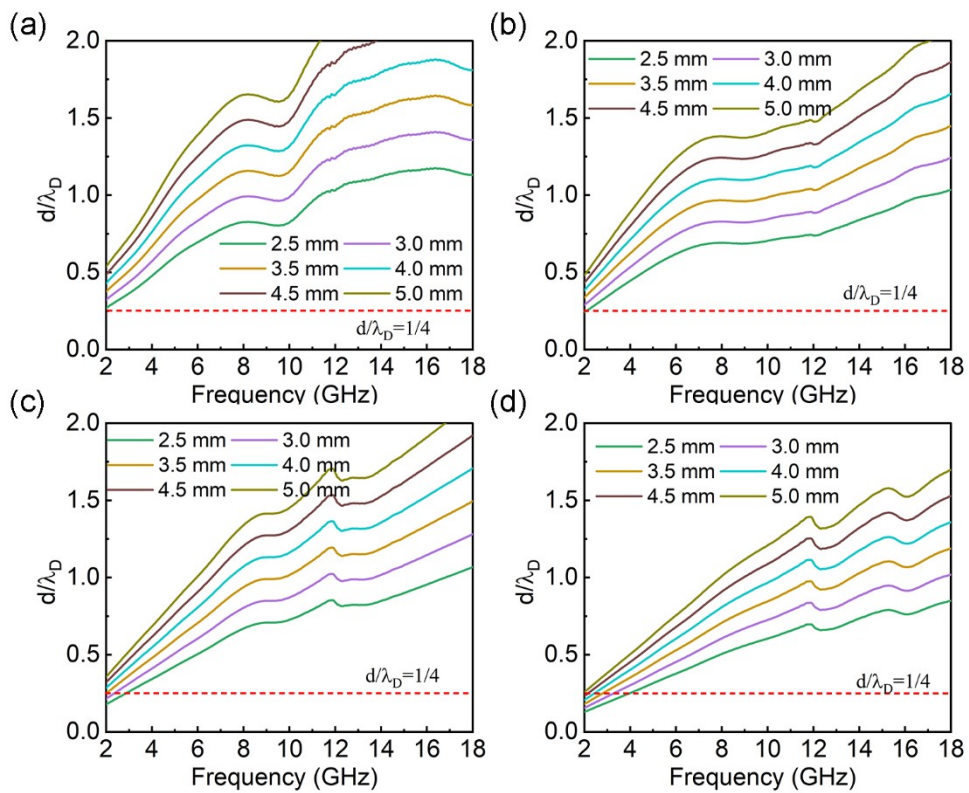


Fig. S8 Frequency dependence of d/λ_D (a) SN-800, (b) SN-1350, (c) SN-1450, and (d) SN-1550.

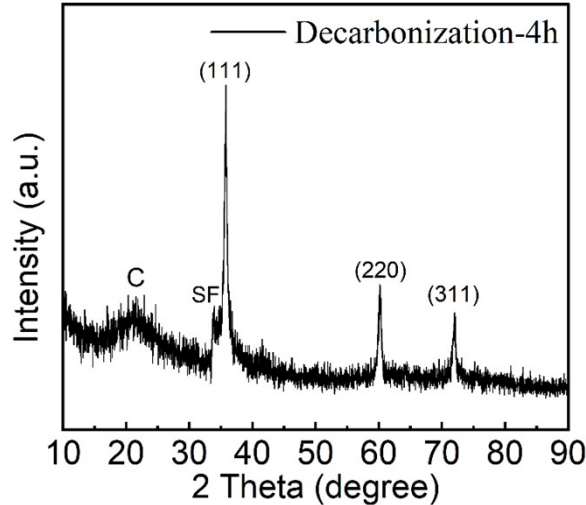


Fig. S9 XRD of Decarbonization-4h.

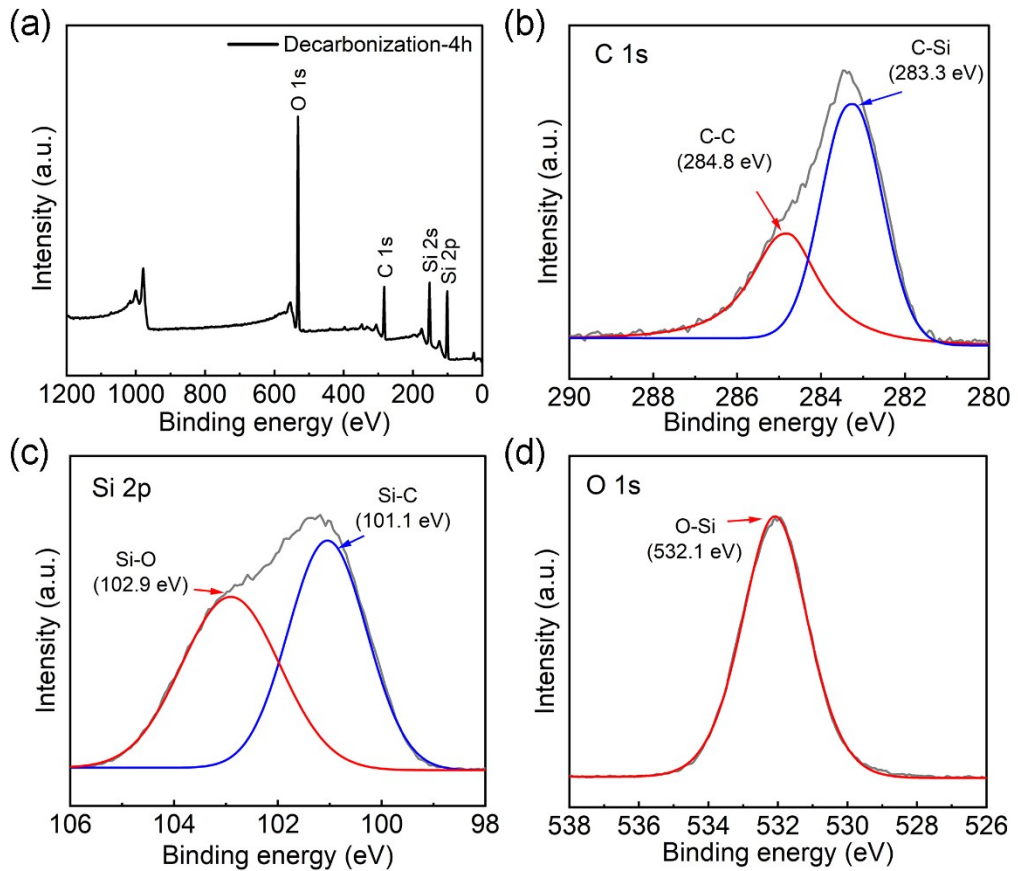


Fig. S10 (a) XPS survey spectra and (b) C 1s, (c) Si 2p, and (d) O 1s regions of Decarbonization-4h.

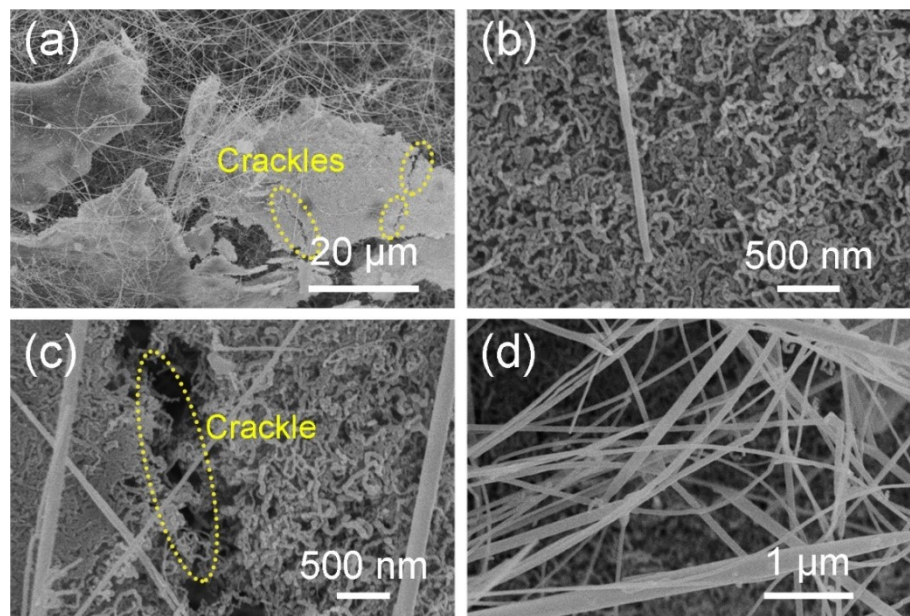


Fig. S11 SEM images of Decarbonization-4h.

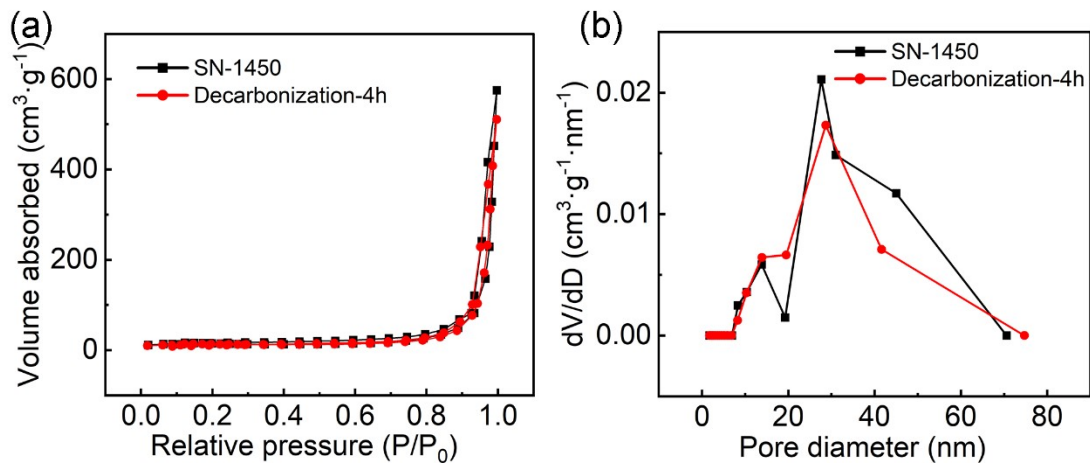


Fig. S12 (a) N₂ adsorption–desorption isotherms at 77 K and (b) pore size distributions of SN-1450 and Decarbonization-4h.

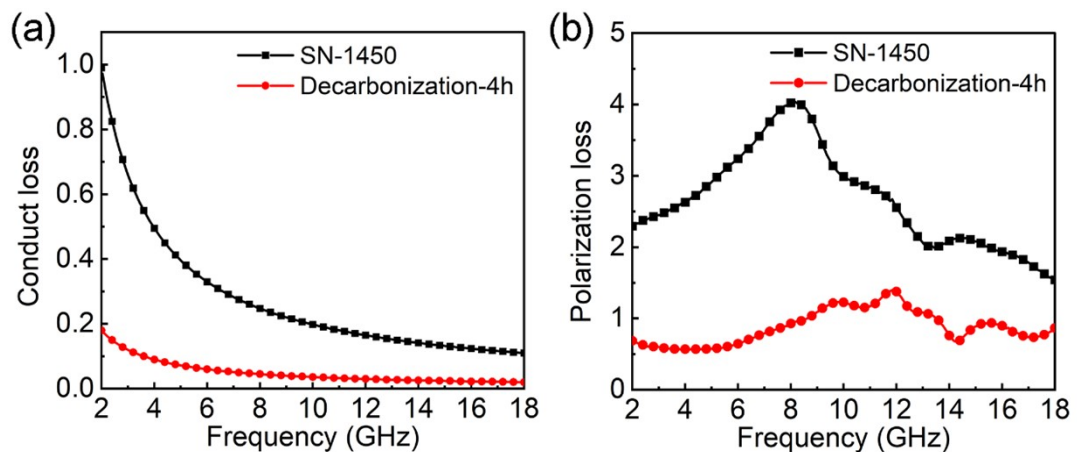


Fig. S13 Comparison of (a) conduction loss (ϵ_c''), and (b) polarization loss (ϵ_p'') for SN-1450 and Decarbonization-4h.

Table. S2 Summary of EMW absorption performance of other relevant studies.

Sample	EAB _{max} (GHz)	Thickness (mm)	The EAB _{max} at a normalized thickness of 4.3mm (GHz)	Reference
Polydopamine-MXene-polydopamine	3.1	1.5	8.88	1
CNT/Cement	12.8	25	2.20	2
Fe ₃ O ₄ @C@NiO	9.9	4.9	8.69	3
Carbon matrix composites	4.64	3.1	6.44	4
CF/CoNi@C/TPU	4.81	2.14	9.66	5
η-MoC/Co@NC-800	4.85	2.5	7.88	6
SiC/MWCNTs	3.34	1.5	9.57	7
Co@C and MXene	4.1	2.5	7.05	8
Co/MnO@NC	6.32	3.5	7.76	9
WS ₂	4.72	3.19	6.36	10
This work	11.04	4.3	11.04	

Reference

- 1 Z. Zhang, A. Chen, X. Li, R. Li, H. Zhou, Z. Liu, X. Zhang, X. Jing, Z. Lin, D. Zhou, B. Kong and L. Xie, *Advanced Functional Materials*, 2025, 2420702.
- 2 X. Wang, Q. Li, H. Lai and S. Xu, *Carbon*, 2025, **234**, 120018.
- 3 X. Wang, H. Zhu, B. Cao, J. Qu, P. Yan and T. Liu, *Small*, 2025, **21**, 2410308.
- 4 J. Wang, S. Zhong, M. Liu, R. Zhang, X. Liu, Y. Huang, X. Liu, X. Wang, D. Lv and L. Xia, *Carbon*, 2024, **229**, 119508.
- 5 Z. Cheng, S. Wang, J. Zhou, J. Yan, Y. Liu, J. Tao, Z. Liu, L. Duan, Y. Yan, J. Yao, Y. Wang, W. Wang, Z. Yao and Y. Ma, *Chemical Engineering Journal*, 2024, **502**, 157810.
- 6 T. Liu, Y. Zhang, C. Wang, Y. Kang, M. Wang, F. Wu and W. Huang, *Small*, 2024, **20**, 2308378.
- 7 Y. Xia, Z. Zhang, K. Li, S. Zhao, G. Chen, Z. Fei, X. Li, Z. Gan, X. Li and Z. Yang, *Chemical Engineering Journal*, 2024, **486**, 150417.
- 8 J.-Z. Chen, P.-P. Chen, B.-Y. Lei, Y.-L. Hou, Z.-A. Li, J.-T. Lei and D.-L. Zhao, *Carbon*, 2024, **230**, 119628.
- 9 B. Wang, F. Huang, P. Zhang, F. Liu, S. Li and H. Zhang, *Carbon*, 2024, **230**, 119633.
- 10 J. Wang, Y. Wang, J. Cheng, Y. Fu, Y. Li, W. Nie, J. Wang, B. Liu, D. Zhang, G. Zheng and M. Cao, *Journal of Materials Science & Technology*, 2024, **194**, 193–202.